Fe-Filled Carbon Nanotubes: Nano-electromagnetic Inductors

P. C. P. Watts,[†] W. K. Hsu,*[,†] D. P. Randall,[‡] V. Kotzeva,[§] and G. Z. Chen[§]

School of Chemistry, Physics and Environmental Science, University of Sussex, Brighton BN1 9QJ, U.K., School of Biological Sciences, University of Sussex, Brighton BN1 9QG, U.K., and Department of Materials Science & Metallurgy, University of Cambridge, Cambridge CB2 3QZ, U.K.

Received August 8, 2002
Revised Manuscript Received September 23, 2002

Carbon nanotubes (CNTs), produced by the catalytic pyrolysis of hydrocarbons, commonly contain metal particles.[1] The encapsulated particles however do not influence the CNT conductivity due to (a) the amount and size of metal particles in CNTs being very small, (b) particles often being present at tube tips[1] and therefore not contributing to CNT conduction, and (c) the electron transfer between the encapsulated metal particles and outer carbon walls being difficult, as a result of 3.4-Å layer separation along the *c*-axis.[2] Recently, Rao et al. successfully produced Fe-filled CNTs;[3] in particular, long Fe single crystals (10−500 nm) are frequently present along the CNT axis (Figure 1a, arrows).[4] Meanwhile, it was found that the ferromagnetic Fe nanocrystals (a) enhance the magnetic coercivities[4] and (b) are protected by CNT walls from oxidation. In fact, the individual chiral CNTs are reminiscent of solenoids,[5] which, in theory, should exhibit an electromagnetic induction (i.e., EMF) when a current is passed through CNTs. Nevertheless, previous alternating current (ac) impedance measurements did not detect an inductive phase in CNTs,[6] which is possibly due to (a) the relatively small portion of chiral tubes in the overall CNT sample, (b) chaotic arrangements of CNTs (cancellation effect), (c) large diamagnetic carbon walls,[7] and (d) insufficient winding turns, e.g., a 45° chiral CNT (5-μm long and 20 nm in diameter) would have less than 70 winding turns. The magnetic field (B) inside the CNT solenoids can be enhanced by the presence of Fe core, according to the equation of $B = B_0 + \mu M$ (B_0, the applied field; μ, the magnetic dipole moment of encapsulated Fe; M, the magnetization of Fe), which is similar to an electromagnet and the magnetic field in CNTs increases. The inductance is (L) $= N\Phi_B/i$, where i is the current, and the magnetic flux linkages of an inductor ($N\Phi_B$) = (nl)(BA), where n is the number of turns per unit length, l the length of an inductor, and A the cross-section area. The above

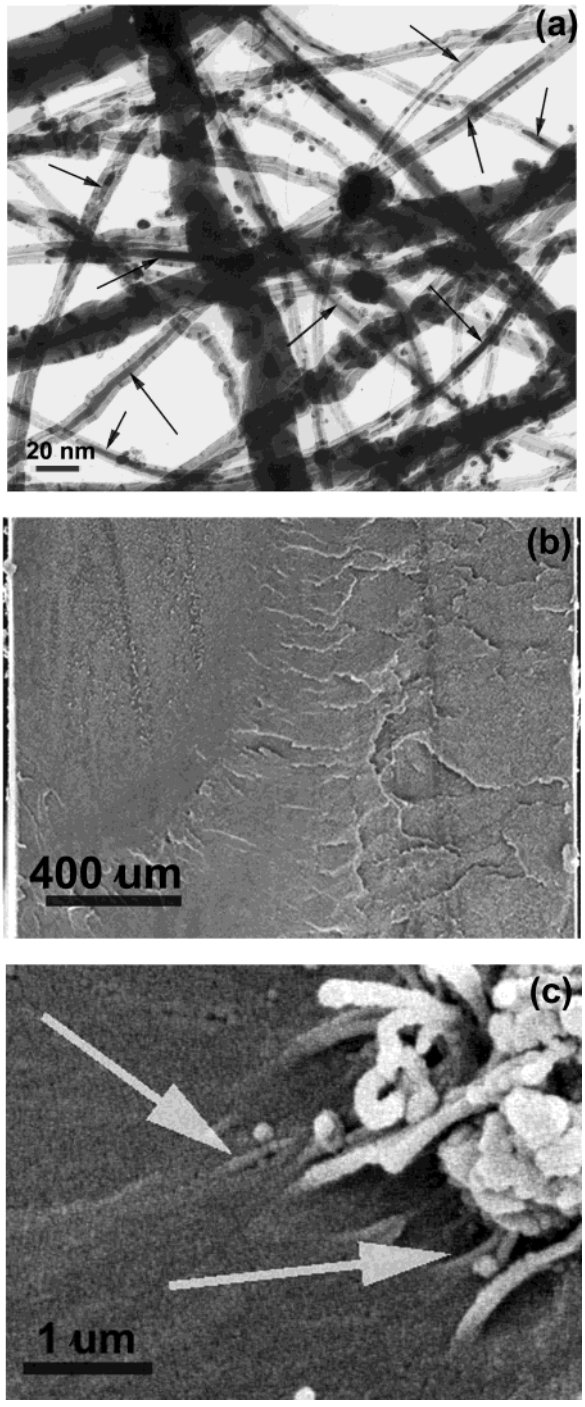

Figure 1. (a) TEM image of Fe-filled CNTs; arrows indicate the encapsulated Fe nanowires. (b) Low-magnification SEM image of an Fe-filled CNT:PS film (1:4). (c) High-magnification SEM image of an Fe-filled CNT:PS film (1:4); arrows indicate the embedded Fe-filled CNTs.

* To whom correspondence should be addressed. E-mail: w.hsu@sussex.ac.uk. Fax: ++44 1273 677196. Tel: ++44 1273 877375.
[†] School of Chemistry, Physics and Environmental Science, University of Sussex.
[‡] School of Biological Sciences, University of Sussex.
[§] University of Cambridge.

(1) Amelinckx, A.; Zhang, X. B.; Bernaerts, D.; Zhang, X. F.; Ivanov, V.; Nagy, J. B. *Science* **1994**, *265*, 635.
(2) Frank, S.; Poncharal, P.; Wang, Z. L.; Heer, W. A. D. *Science* **1998**, *280*, 1744.
(3) Rao, C. N. R.; Sen, R.; Satishkumar, B. C.; Govindaraj, A. *Chem. Commun.* **1998**, *15*, 1525.
(4) Grobert, N.; Hsu, W. K.; Zhu, Y. Q.; Hare, J. P.; Kroto, H. W.; Walton, D. R. M.; Terrones, M.; Terrones, H.; Redlich, Ph.; Rühle, M.; Escudero, R.; Morales, F. *Appl. Phys. Lett.* **1999**, *75*, 3363.
(5) Miyamoto, Y.; Louie, S. G.; Cohen, M. L. *Phys. Rev. Lett.* **1996**, *76*, 2121.
(6) Yang, Z. H.; Wu, H. Q. *Chem. Phys. Lett.* **2001**, *343*, 235.
(7) Ramirez, A. P.; Haddon, R. C.; Zhou, O.; Fleming, R. M.; Zhang, J.; McClure, S. M.; Smalley, R. E. *Science* **1994**, *265*, 84.

10.1021/cm021288p CCC: $22.00
Published on Web 10/30/2002

equations clearly indicate the enhancement of magnetic flux linkages inside CNT solenoids via the encapsulation of Fe crystals. We therefore believed that if an ac is passed through these Fe-filled CNTs, the induction profile might appear in ac impedance spectra. In this communication, the ac impedance technique is employed to probe the electronic properties of Fe-filled CNT−polystyrene (PS) composites. Surprisingly, we find that composite films exhibit the resistive, capacitive and inductive phases, as materials were measured from high frequency to low frequency. The presence of inductive phase in CNT−polymer composites is novel because an electrically conducting CNT−polymer composite commonly exhibits resistive and capacitive characteristics only;[8] the former originates from CNT resistors and the latter from the dielectric polymer matrix and localized bilayer capacitive structures (e.g., CNT/polymer/CNT).[9] Our study reveals that the presence of induction behavior in Fe-filled CNT−PS composite films is actually due to the electromagnetic phenomenon associated with the encapsulated Fe nanocrystals in the CNTs, not self-inductance from the electrical leads and instruments (i.e., stray inductance).

The Fe-filled CNTs were produced by the pyrolysis of ferrocene at 1000 °C in the presence of Ar flow, as described previously.[3,4] Fe-filled CNT−PS composite films were made by a solvent-vacuum-casting technique,[10] followed by a hot-pressing process to remove the residual solvent and to minimize the internal voids of the film.[10] The CNT-to-polymer ratio (wt. %) varies from 1:2 to 1:6 and composite films (30 × 15 × 2 mm) were marginally silver painted to maintain electrical connections for the two-terminal ac impedance tests from 1 MHz to 0.1 Hz. The ac impedance instrument is a potentiostat (PGSTAT30), equipped with a frequency response analyzer (FRA) module controlled by a PC-free ISA slot.

Figure 1b shows a low-magnification SEM image of a composite film (1:4 ratio). The film thickness is very uniform and the film voids have been minimized. The high-magnification SEM image reveals that the nanocylindrical structures are embedded in the PS matrix (Figure 1c, arrows), presumably Fe-filled CNTs. We notice that high Fe−CNT-loaded composite films (e.g., 1:2−4 ratios) will instantly respond to an external magnetic field. Figure 2a shows a graph of impedance module $|Z|$ versus frequency (Hz) for the Fe-filled CNT:PS (1:2) composite film, where the $|Z| = (Z'^2 + Z''^2)^{1/2}$ and Z' and Z'' represent the real and imaginary impedances, respectively. Figure 2a can be divided into three regions (I−III). The impedance module in region (I) remains constant, followed by a small increase in region (II), and then a relatively significant increase in region (III). At low frequencies (region I), the $|Z|$−Hz profile is linear and independent of frequency, i.e., the voltage and current are in phase and the phase separation angle ϕ is zero. In other words, the composite film behaves as a pure resistor in region (I). The resistive phase is also verified by the presence of zero-imaginary impedance

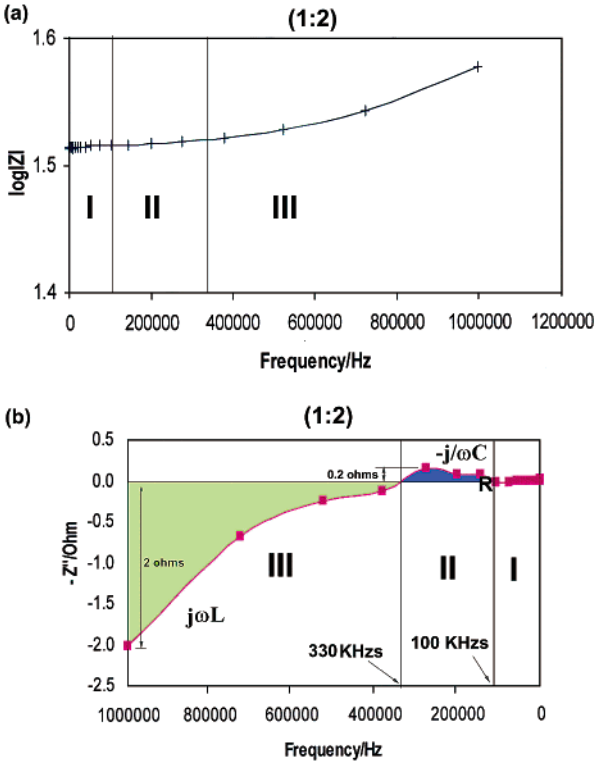

Figure 2. (a) The graph of impedance module versus frequency for the 1:2 film. (b) The graph of imaginary impedance versus frequency for the 1:2 film. Blue and green regions represent the capacitive and inductive reactance, respectively.

shown in Figure 2b (Z'' versus Hz, region I). The total film impedance $Z = R - j/\omega C + j\omega L$ and the angular frequency $\omega = 2\pi f$. The first, second, and third terms represent the resistive, capacitive, and inductive reactance, respectively. If the imaginary impedance is equal to zero, the $-j/\omega C = j\omega L = 0$ and the total film impedance $Z = R$, which is consistent with region (I) shown in Figure 2a. The total film impedance for the 1:2 composite film in region (I) (Figure 2a) is ca. 32.6 Ω, which slightly increases toward the positive region (capacitive phase, Figure 2b) by ca. 0.2 Ω in region (II) (i.e., the transition from resistive to capacitive phase at 100 kHz, Figure 2a,b, right arrow). The small impedance increase in region (II) is neither due to the presence of resistance variation in electrical connections nor the stray capacitance from the instruments because of the following: (a) ac impedance devices exhibit very low contact resistance between the composite film and leads (<0.1 Ω). (b) The peak-to-peak amplitude (i.e., exciting signal amplitude) was constantly kept at a small value (10 mV) in all experiments, which means that the small background noise will be smoothened to a close linear approximation.[11] (c) The Figure 2b (region II) shows that the imaginary impedance Z'' is present in the first quadrant (above the x-axis, blue), i.e., the $-j/\omega C \neq 0$ and $j\omega L = 0$. In other words, the presence of film impedance increase in region (II) is due to the contribution from the capacitive reactance and the total film impedance in region (II) is $Z = R - j/\omega C$. (d) The stray capacitance is commonly present at relatively high

(8) Sandler, J.; Shaffer, M. S. P.; Prasse, T.; Bauhofer, W.; Schulte, K.; Windle, A. H. *Polymer* **1999**, *40*, 5967.
(9) Hughes, M.; Chen, G. Z.; Shaffer, M. S. P.; Fray, D. J.; Windle, A. H. *Chem. Mater.* **2002**, *14*, 1610.
(10) Poa, C. H.; Silva, S. R. P.; Watts, P. C. P.; Hsu, W. K.; Kroto, H. W.; Walton, D. R. M. *Appl. Phys. Lett.* **2002**, *80*, 3189.
(11) Southampton Electrochemistry Group. *Instrumental Methods in Electrochemistry*; Ellis Horwood: London, 1990; ISBN 0-13-472093-8, Chapter 8, pp 251−269.

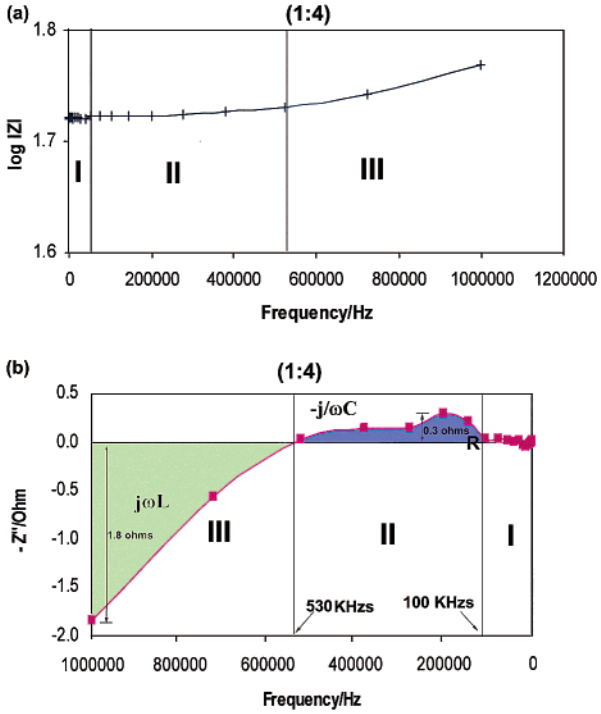

Figure 3. (a) The graph of impedance module versus frequency for the 1:4 film. (b) The graph of imaginary impedance versus frequency for the 1:4 film. Blue and green regions represent the capacitive and inductive reactance, respectively.

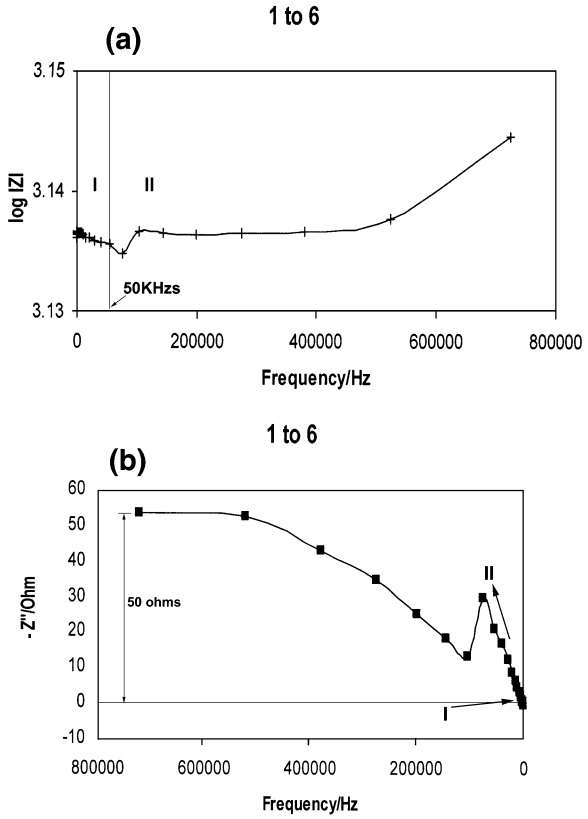

Figure 4. (a) The graph of impedance module versus frequency for the 1:6 film. (b) The graph of imaginary impedance versus frequency for the 1:6 film.

frequencies (>1 MHz)[11] and the observed capacitive phase in region (II) lies in the 100−320-kHz range. Previous reports have pointed out that the capacitive reactance increases with increasing frequency for low CNT-loaded composite films (i.e., high-resistance films);[8] namely, the capacitive phase is mainly due to the sandwiched structure of the lead/polymer/lead. For high CNT-loaded films (i.e., low-resistance films), the capacitive reactance decreases and the sandwiching lead/polymer/lead structure is replaced by the localized bilayer capacitive structures in the films (i.e., CNT/PS/CNT), which accounts for the presence of the capacitive phase in region (II) (Figure 2a,b). The small capacitive reactance increase in region (II) corresponds to 24.8 μFs (capacitance $C = 1/\chi_c\omega$, χ_c; capacitive reactance, Ω), a value which is ca. 3 orders of magnitude lower than those obtained from porous CNT−PPy composites.[9]

The total film impedance continuously increases (by ca. 2 Ω) from region (II) to region (III) at 1 MHz (Figure 2a,b) and interestingly the Z''−Hz plot shows that the imaginary impedance profile transits from the first quadrant (blue) to the fourth quadrant (green) at 330 kHz (Figure 2b, regions II−III, arrow), which means that the inductive reactance (χ_L) begins to contribute to the total impedance of the composite film, i.e., the $-j/\omega C = 0$ and $j\omega L \neq 0$ (Figure 2b, green region). In other words, the total film impedance in region (III) is $Z = R + j\omega L$ and the inductance (L) at 1 MHz is ca. 0.3 μHys ($L = \chi_L/\omega$, χ_L: the inductive reactance, Ω).

Figure 3a,b shows the $|Z|$−Hz profile and Z''−Hz plots for the 1:4 ratio composite film, which are similar to those in Figure 2a,b, i.e., the resistive reactance ($Z = R$) for region (I), resistive + capacitive reactance ($Z = R - j/\omega C$) for region (II), and resistive + inductive reactance ($Z = R + \omega L$) for region (III), respectively. The total film impedance is ca. 52.5 Ω in region (I) and then increased by ca. 0.3 Ω and 1.8 Ω in regions (II) and (III), respectively (Figure 3a). By comparison with Figure 2a,b, several features however can be distinguished. First, the extent of capacitive reactance increase in region (II) is slightly greater than the value obtained in the 1:2 film. Second, the extent of the inductive reactance increase in region (III) is slightly lower than the value obtained in the 1:2 film. Third, the transition from the resistive (i.e., R on the x-axis) to capacitive phase (above the x-axis, blue region) occurs at 100 kHz, similar to that of the 1:2 film. Fourth, the transition from the capacitive to inductive phase (fourth quadrant, green region) occurs at 530 kHz, which is higher than that of the 1:2 film. For the 1:6 film, the inductive phase is absent and the total film impedance originates only from resistive components at very low frequency for region (I) (50 kHz to 0.1 Hz, Figure 4a,b) and a combination of resistive and capacitive components for region (II) (1 MHz to 50 kHz, Figure 4a,b). The total impedance for the 1:6 film in region (I) is ca. 1370 Ω, a value which increases to ca. 1420 Ω in region (II) at 1 MHz (Figure 4a). The extent of capacitive reactance increase in the 1:6 film is greater than the value obtained for the 1:2 and 1:4 films.

According to Figures 2−4, it is clear that the capacitive reactance (χ_c) increases with embedded Fe−CNT content decreasing, as consistent with reports.[8] The factor that is responsible for the relationship between the capacitive reactance and CNT content is as follows. When the CNT load in the PS matrix decreases, more localized bilayer capacitive structures are created due to an increase in the gap among adjacent CNTs (e.g., 1:2 → 1:4 films). Further reduction of CNT load leads

to capacitive structures transition from the localized CNT/polymer/CNT to lead/PS/lead phase (1:4 → 1:6, previously defined as CNT percolation threshold by others),[8] as the frequency increases. At low frequencies, the electrical conduction through the capacitive-like structures is primarily diffusion type, i.e., the electron tunneling from tube to tube. It is unlikely that the Warburg impedance (i.e., low frequency-dependent resistance, <500 Hz) is involved in film circuit elements because the capacitive phase begins at ca. 100 kHz for 1:2 and 1:4 films and 50 kHz for the 1:6 film (Figure 4b). The electron-hopping mechanism dominates at high-frequency regions because the diffusion process is unable to immediately respond to ac excitation at high frequencies.[11] The diffusion-hopping transition is supported by the presence of a hump at ca. 100 kHz in the 1:6 film (Figure 4b). In fact, humps are also present in the capacitive region (II) (Figures 2b and 3b). For example, the hump is present at ca. 200 and 300 kHz for 1:4 and 1:2 films, respectively, which means that high CNT-loaded films allow the occurrence of a diffusion-hopping transition at higher frequencies. This phenomenon is due to the fact that the gap among adjacent CNTs significantly decreases at high CNT-loaded films, which facilitates the electron-tunneling process.

The origin of the inductive phase in impedance profiles is truly from composite films based on the following: (a) The inductive reactance decreases with Fe content decreasing (1:2 → 1:4) and the induction is absent in the 1:6 film. (b) If the induction arises from the electrical leads, one would expect that all ac impedance tests of composite films should have an accompanying induction signal, irrespective of Fe content. (c) Less Fe content in the film will require higher frequencies to induce EMFs, which is consistent with $Z''-$Hz plots (Figures 2b and 3b); the inductive phase occurs at 330 kHz for the 1:2 film and 530 kHz for the 1:4 film. (d) The stray inductance is commonly present at very high frequency regions (>1 MHz).[11] (e) Composite films, made by mixing CNTs, Fe (or Fe_3O_4) powder, and PS, do not show an inductive phase, which means that only encapsulated Fe crystals are capable of enhancing the magnetic field inside CNT solenoids. (f) The inductive reactance increases with frequency increasing (e.g., Figure 2b) due to $\chi_L = \omega L$, which further verifies the origin of induction from the films. It is therefore clear that the inductive phase seen in region (III) (Figures 2a and 3a) is attributed to the electromagnetic induction associated with the ferromagnetic Fe core in CNTs. The absence of inductive phase in the 1:6 film is actually due to the fact that ac impedance tests were limited below 1 MHz. As mentioned above, less Fe content in the film requires higher frequencies to generate an inductive phase, which means that the 1:6 film would need to exceed 1 MHz for producing an induction phenomenon.

Pyrolysis of ferrocene also generates Fe-encapsulated carbon nanoparticles. However, a previous study showed that the conduction pathway within the polymer matrix is via CNT percolation,[12] which implies that Fe-encapsulated carbon particles are not involved in the generation of electromagnetic induction. Accordingly, the specific capacitance and inductance of composite films is difficult to be evaluate.

Acknowledgment. We thank the Leverhulme Trust and Wolfson Foundation of UK for financial support.

CM021288P

(12) Watts, P. C. P.; Hsu, W. K.; Chen, G. Z.; Fray, D. J.; Kroto, H. W.; Walton, D. R. M. *J. Mater. Chem.* **2001**, *11*, 2482.